Appl. Phys. B 63, 331–337 (1996)

Applied Physics B Lasers and Optics

ODMR and EPR investigations of Fe centers in $KTaO_3$

H.-J. Reyher, B. Faust, M. Maiwald, H. Hesse

FB Physik, Universität Osnabrück, D-49069 Osnabrück
(Fax:+49-541-9692670, E-mail: hjreyher@physik.uni-osnabrueck.de)

Received: 8 May 1996 / Accepted: 5 July 1996

Dedicated to O. F. Schirmer on the occasion of his 60th birthday

Abstract. The analysis of EPR spectra obtained from iron doped $KTaO_3$ crystals in the as-grown state revealed three dominant iron centers: Fe^{3+}-O_I, axial Fe-centers with spin $S = \frac{3}{2}$ and rhombic Fe^{3+}. By comparison with data from literature possible assignments for the center with $S = \frac{3}{2}$ are discussed. For the rhombic species the temperature dependence of the main parameters of the Spin- Hamiltonian was measured. The result makes it most plausible that only one rhombic iron center exists in $KTaO_3$, in contrast with literature. The understanding of the EPR spectra allows us to assign transitions, observed at very low magnetic fields by optically detected magnetic resonance (ODMR), to this rhombic Fe center. On this basis, the magnetic circular dichroism (MCD) of this defect could be identified using the method of tagged-MCD. This spectrum is compared to the tagged-MCD of Fe^{3+}-O_I and of axial Fe^{4+} centers, which may be generated metastably by optical charge transfer. Considerably different structures in the MCD spectra of both Fe^{3+} centers indicate different local surroundings and electronic states.

PACS: 76.30.Fc; 76.70.Hb; 78.20.Ls

Most of the electro-optical applications using oxide materials are based upon processes being determined in a decisive way by point defects [1]. As a rule, extrinsic defects are most important, specifically those formed by intentional or fortuitous doping by ions from the group of transition elements. To optimize crystals for a specific application hence requires to understand the nature of these centers. Electron paramagnetic resonance (EPR) in combination with optical methods proved to be well suited to attain such knowledge for, e.g., $LiNbO_3$, $BaTiO_3$, and $KTa_{1-x}Nb_xO_3$ [2]. Chemically and structurally related to these substances is $KTaO_3$, a cubic, centrosymmetric crystal, showing no phase transitions [3], and therefore being unsuited for electro-optical applications. Nevertheless, there is enormous interest in the properties of this substance, mainly because of two reasons. First, $KTaO_3$ exhibits a strong increase of the dielectric polarizibility with falling temperature, which has lead to the label 'incipient ferroelectric' and stimulated investigations concerning the role of symmetry breaking impurities like lithium or niobium [4, 5]. Second, one may consider $KTaO_3$ as a model material, which is easier accessible to investigations at low temperatures where related substances exhibit phase transitions and may show multi-domain structure.

The latter point is of particular importance in studies of the optical absorption via the magnetic circular dichroism, MCD. If combined with paramagnetic resonance, then being called optically detected magnetic resonance (ODMR), one arrives at the method of 'tagged-MCD', known to be able to attribute absorption bands to specific impurities in a compelling way [6]. The latter aspect is the main goal of our work. Poly-domain structured crystals, like $BaTiO_3$ at the temperatures required for these methods, do not allow the MCD to be measured, since the polarization of the probe light is destroyed by scattering at the domain boundaries. Even if the non-cubic relatives of $KTaO_3$ are mono-domain, the presence of a strong linear birefringence often substantially complicates MCD-ODMR experiments. On the other hand it would be highly desirable to identify the impurities that are responsible for the optical absorption in the materials used for electro-optical applications. Absorption may either be unwanted, as in the case of, e.g., light modulators, or fundamentally necessary, as in the photorefractive effect, where it represents the primary step [1]. We therefore want to clarify the nature of absorption bands in $KTaO_3$ and assume that the results obtained there may be transferred to similar materials. The combination with EPR will allow to draw more precise conclusions than it is possible from purely optical methods (see, e.g., Ref.[7]).

Iron is very often found in the oxides in question, and is frequently regarded as a 'good candidate' whenever defects are seen to be responsible for one effect or another. A number of EPR-related investigations on iron centers in $KTaO_3$ is described in literature, both for doped and nominally pure material. Already in early work three sites of different point symmetry for Fe^{3+}-ions were reported [8, 9], cubic sites, where iron substitutes for Ta- as well as for K-ions, sites having axial (tetragonal) and rhombic symmetry. Later, the

temperature shift of the cubic crystal field parameter a of Fe^{3+}_{Ta} was analysed and related to ferroelectricity by comparison to other oxides [10]. In that work also the influence of annealing procedures on the relative strengths of axial and cubic iron spectra was mentioned, which was later examined in more detail [11, 12]. Further examinations showed the existence of two types of axial Fe^{3+} centers [13]. The nature of these centers with $S^{eff} = \frac{1}{2}$, $g_{\perp}^{eff} \approx 6$, $g_{\parallel}^{eff} \approx 2$ at X-band frequencies, which we shall furtheron call Fe6/2 centers, was proposed to be Fe^{3+}_{Ta}-V_O and Fe^{3+}_{K}-O_I. This identification was confirmed by studies of the influence of redox-treatments on the relative center concentrations [14] and by theoretical work [15]. Recently, we have reported on the optical alignment of Fe^{3+}_{K}-O_I centers [16]. A further axial center, with effective spin $S^{eff} = \frac{1}{2}$, $g_{\perp}^{eff} = 4.33$, $g_{\parallel}^{eff} = 2$ (Fe4/2 center), has been attributed to Fe^{3+} [17] and later to Fe^{+}_{K} [18, 19, 20]. Finally, a complete analysis of the angular dependence of the spectrum from rhombic iron (rhFe centers in the following) was given at room temperature [21]. This center has then been assumed to be in correlation with the existence of ferroelectric microregions in $KTaO_3$ [22]. Recently, a similar spectrum observed at 4.2 K led to the conclusion that a second rhFe center exists in $KTaO_3$ [23]. However, we will show below that the observed difference between the spectra arises from a temperature shift of the crystal field parameters of a single center. In view of the complex defect scenario in iron doped $KTaO_3$, we will confine ourselves on as-grown material and the mentioned iron centers.

1 Experimental

Several $KTaO_3$ crystals have been studied, which were iron doped by adding 0.25, 0.5 and 2 mol% Fe_2O_3 to the melt. The Fe-concentration in the crystals has not been determined, but iron is known to be easily incorporated in $KTaO_3$. All specimens were grown in air by the top-seeded-solution-growth method at the University of Osnabrück. The yellow-brownish color of the samples was the darker the higher the Fe-content.

Conventional EPR was performed using a Bruker CW spectrometer at X- and Q-band frequencies (9 and 35 GHz), equipped with an Oxford evaporation cryostat for low-temperature measurements. MCD of absorption, ODMR via the MCD of absorption and tagged-MCD were measured using a conventionally designed system consisting of an Oxford 3 T magnet-cryostat, Q- and E-band (70 GHz) microwave equipment and an optical setup suited for MCD spectroscopy (xenon arc-lamp, monochromator, elasto-optical modulator, photomultiplier) [6, 24].

2 Results and Discussion

First we discuss our results from EPR measurements, since these findings form the basis for the identification of the observed ODMR spectra. This identification allows then to interprete the tagged-MCD spectra shown in subsection 2.2.

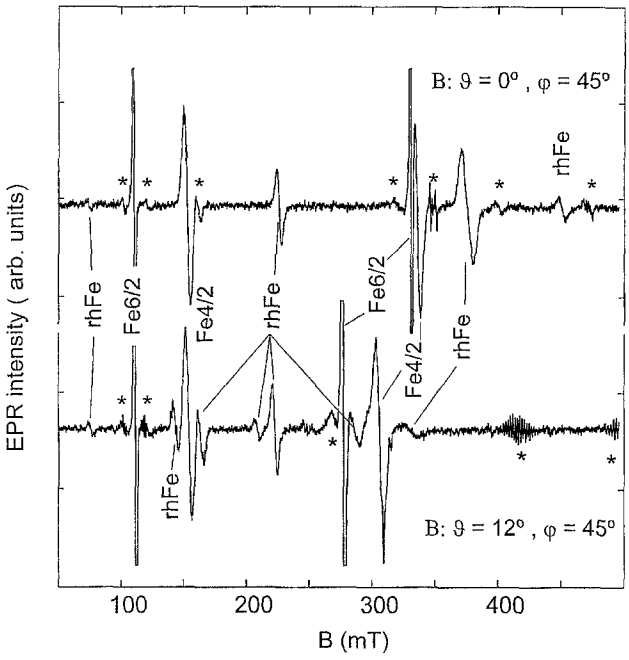

Fig. 1. Typical X-band EPR-spectrum of as-grown $KTaO_3$:Fe (0.25 mol%) at T = 75 K, 9.26 Ghz. The orientation of **B** is given by the azimuthal and polar angles with respect to the cubic system. Asteriks mark resonances that are not yet identified

2.1 Conventional EPR

As grown, all the specimens showed very similar EPR spectra containing in each case the lines from Fe6/2, Fe4/2 and rhFe. The Fe6/2 centers were dominating, with one exception, where rhFe showed the strongest lines. In some cases Gd^{3+} on a cubic site was found as unintended dopant [18, 19, 25], cubic Fe^{3+} spectra have never been found in our as grown material. Figure 1 shows typical EPR spectra obtained at 75 K, the upper trace for the case **B** $\parallel$ [001] and the lower one for $\vartheta \approx 12°, \varphi \approx 45°$. Here, ϑ and φ are defined in the conventional sense as the polar and azimuthal angle with respect to [001] and [100]. The resonances are labelled according to the results of measurements of angular dependences. Some not yet identified features are marked by asteriks. In Fig. 2 the angular dependence of B_{res} of the major lines is shown for a rotation around [010] and around a [$\bar{1}$10]-direction. Most of the data points can be associated to transitions of rhFe and the axial iron centers Fe6/2 and Fe4/2. Fits to these data were performed by *R-Spectr* [26], a program collection performing numerical diagonalization of the appropriate Spin-Hamiltonian.

Table 1 lists the parameter values obtained in this way. Since the effective spin parameters at X-band frequencies are practically identical for both Fe^{3+}_{Ta}-V_O and Fe^{3+}_{K}-O_I, we also performed control measurements at 34 GHZ, by which both centers can clearly be distinguished [13]. The Fe6/2-center is therefore attributed to Fe^{3+}_{K}-O_I in Table I. In contrast with this, Fe4/2 is not assigned to a specific ion, since there are problems when comparing with published Fe4/2-results [17, 18, 19, 20]. Our values agree with those given in Ref. [17], where the resonances are attributed to either axial Fe^{3+} or Ni^{3+}. Since we never observed the usual Ni-spectra [8] in our iron doped samples, we prefer the attri-

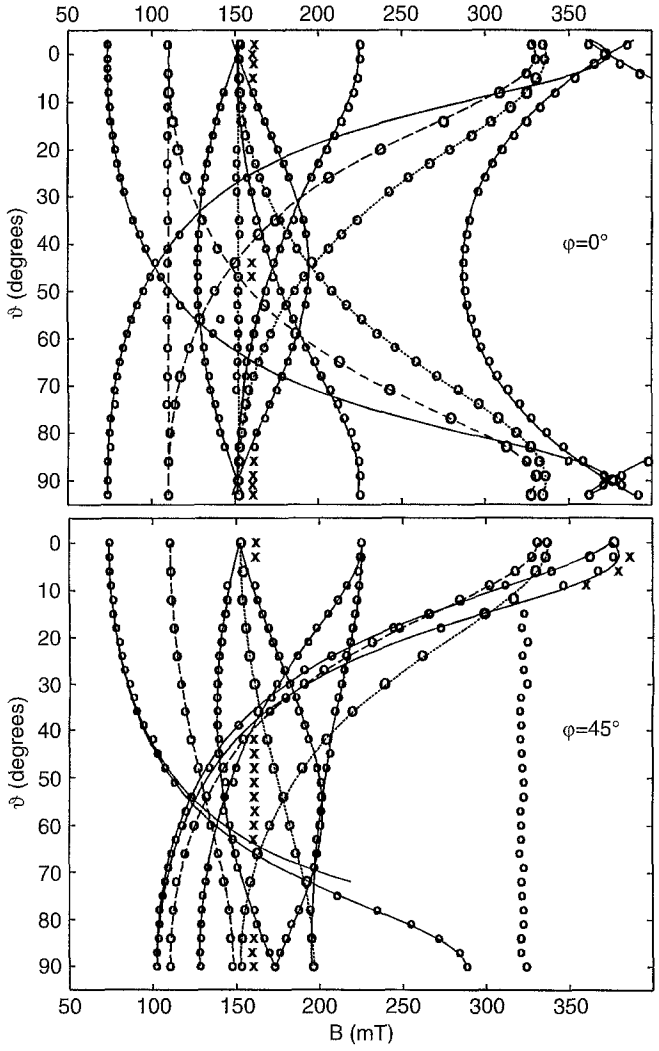

Fig. 2. Angular dependence of the main lines shown in Fig. 1 for rotations of **B** around [010] (top) and [$\bar{1}$10] (bottom). The experimental points are weighted by the observed resonance intensity, the lines are results of a fit to the lower part. Straight lines: rhFe, dotted: Fe4/2, dashed: Fe6/2. Unidentified resonances are marked by 'x'. The data points at 320 mT are due to Gd^{3+}

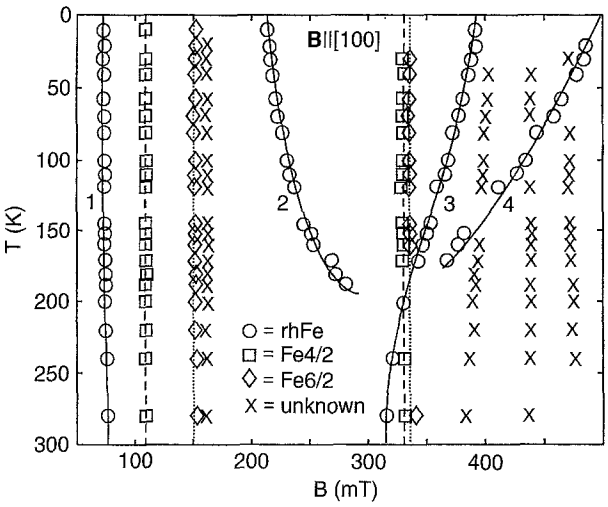

Fig. 3. Resonance fields of EPR transitions from rhFe, Fe4/2, Fe6/2 and some unidentified species as a function of temperature. The lines are guides to the eye. **B** || [001], 9.22 GHz

bution to iron ions. However, the charge state (3+) is unlikely, since $g^{eff} = 4/2$ rather fits to axial iron with $S = \frac{3}{2}$. Therefore, Fe^{+} and Fe^{5+} have been discussed as sources of resonances with $g^{eff} = 4/2$ in $KTaO_3$ [18, 19]. Using formulas from Ref. [27], the authors argued that, since the true g-values ($S = \frac{3}{2}$) are both larger than $g^{free} = 2.0042$ ($g_{\|} = 2.02, g_{\perp} = 2.16$), only Fe^{+} should be acceptable. However, this argumentation may not be sufficient, since in a later publication $g_{\|}$ of Fe^{+} was given as 2.00(2) [20], a values which agrees with with our finding for Fe4/2 [28]. A small negative $\delta g_{\|}$ for a d^7-configuration may be explained by referring to more refined theory [29], as shown in Ref. [30]. These authors could explain the observed g-shifts of Fe^{+}-V_O in $SrTiO_3$ ($g_{\|} = 1.999, g_{\perp} = 2.058$) assuming reasonable values for the parameters of the theory applied. For axial Fe^{5+} in the same crystal, on the other hand, positive values for both $\delta g_{\|}$ and $\delta g_{\perp}$ have been found [31], whereas the simple formula used in Refs. [18, 19] would predict negative shifts for the d^3-configuration of this ion. Since obviously there exists still the problem of explaining the g-values of Fe4/2 satisfactorily, we do not want to assign our Fe4/2 signals to either Fe^{+} or Fe^{5+} without further work.

The parameters found for rhFe at 75 and 290 K are similar to those that have been attributed to Fe^{3+} on orthorhombically distorted K- and Ta-sites, respectively [21, 23]. However we will show below, that both parameter sets belong to only one rhFe center.

Before doing so, we want to stress on the unusually great number of resonance features in the spectra. Indeed, several minor lines are not included in Fig. 2, since, unfortunately, only parts of the corresponding branches could so far be distinguished from the known ones. Examples for these unknown resonances are marked by crosses, among those, most interestingly, an isotropic line at $g^{eff} = 4.11$. Also the satellite lines of the Fe6/2, showing up in Fig. 1 at 101 mT and 120 mT, are omitted from Fig. 2. The fact that these lines, which can savely be identified only below ≈150 mT, follow the Fe6/2 branches, suggests that they result from $^{57}Fe^{3+}$-O_I, but this has to be checked more thoroughly. Finally, the isotropic line, shown only in the lower part of Fig. 2, is due to Gd^{3+} [25], the fine-structure being not resolved in this scale.

Next we want to clarify the question, which of the rhFe centers described in literature should be present in our samples. The answer to this question is complicated by the fact, that it was mentioned in Ref. [23] that the parameters of rhFe on the K-site should depend on temperature. The MCD/ODMR signals of rhFe at 2 K, to be presented below, may well be explained with a parameter set for the Spin-Hamiltonian of the $rhFe_K$, observed at 4.2 K by EPR [23]. The ODMR results do *not* agree with the T-independent [23] values of $rhFe_{Ta}$ evaluated at 300 K [21]. As we found values for rhFe at room temperature that are, within error, compatible with those from Ref. [21], one had to concluded that $rhFe_{Ta}$ is not to be observed by MCD/ODMR. To solve this problem we measured the two most important parameters of the Spin-Hamiltonian of rhFe as a function of temperature. A determination of all eight possibly significant parameters of the Spin-Hamiltonian for rhFe would require measure-

Table 1. Values of Spin-Hamiltonian parameters. '*' refers to this work. For the tetragonal centers Fe6/2 and Fe4/2 the 4-fold axis is along [100], for rhFe the 2-fold z-axis is along [110]. Equivalencies: $b_{20} = D$, $b_{22} = 3E$, $b_{4i} = 60B_{4i}$. Symmetry and orientation of the rhFe centers is sketched in Fig. 5.

center	Ref.	remarks	g factor	crystal field (CF), second order (cm^{-1})	CF, fourth order (cm^{-1})
Fe6/2	*		values identical with [13], checked at 34 GHz		
	[13]	Fe^{3+}-O_I	$g_{\|} = g_{\perp} : 2$	$b_{20} : 4.46$	
Fe4/2	*	$S_{eff} = \frac{1}{2}$	$g_{\perp,\|} : 4.34(3), 1.96(1)$		
	[19]	Fe^{+}_{K}	$g_{\perp,\|} : 4.33, 2.02$		
	[20]	Fe^{+}_{K}	$g_{\perp,\|} : 4.33(1), 2.00(2)$		
	[17]	Fe^{3+}/Ni^{3+}	$g_{\perp,\|} : 4.337(2), 1.968(2)$		
rhFe	*	$Fe^{3+}_{?}$, 290 K	$g_{x,y,z} : 2.00(1), 2.00(1), 2.00(1)$	$b_{20,22} :$ 0.434(10), 0.178(10)	$\|b_{4i}\| < 0.02$, not significant
	*	$Fe^{3+}_{?}$, 75 K	$g_{x,y,z} : 1.99(1), 2.00(1), 2.00(1)$	$b_{20,22} :$ 0.475(10), 0.254(10)	$\|b_{4i}\| < 0.02$, not significant
	[23]	Fe^{3+}_{Ta}, 4.2 K	$g_{x,y,z} : 1.990, 1.996, 1.998$	$b_{20,22} :$ 0.474, 0.276	$b_{40,42,44} : -2 \cdot 10^{-4}$, $2.1 \cdot 10^{-4}, 1.1 \cdot 10^{-2}$
	[21]	Fe^{3+}_{K}, 300 K	$g_{x,y,z} : 1.99, 2.01, 2.00$	$b_{20,22} :$ 0.44, 0.196	$b_{40,42,44} : 1.9 \cdot 10^{-4}$, $1.7 \cdot 10^{-2}, 1.8 \cdot 10^{-2}$

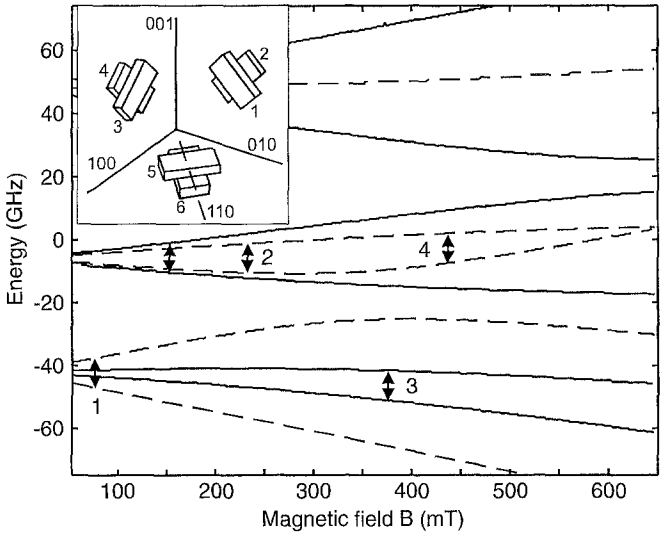

Fig. 4. Level diagram of rhFe drawn using the parameters from Tab. 1 for 75 K, **B**||[001]. Transitions are shown for 9.28 Ghz, the labels refer to the branches from Fig. 3. For the given orientation one has two magnetically inequivalent sites represented by centers 1-4 and 5+6 (see inset), leading to the dashed and straight lines, respectively

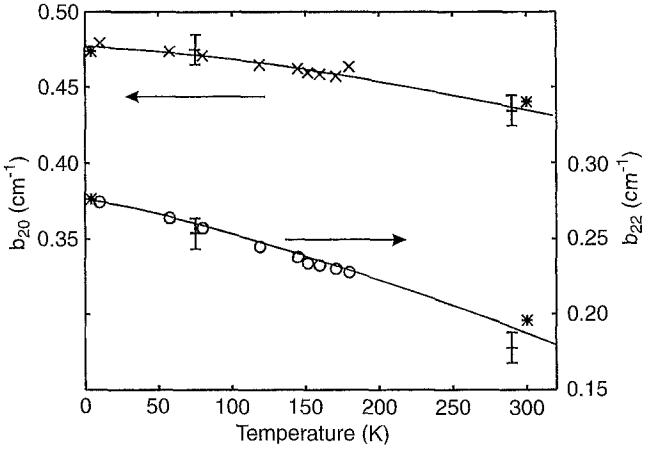

Fig. 5. Spin-Hamiltonian parameters b_{20} and b_{22} of rhFe as a function of temperature. 'x': b_{20} from fits to four transitions for **B** || [001] (see text), 'o': the same for b_{22}, '*': Refs. [21, 23], 'error-bar': fit to angular dependences, this work. The lines are guides to the eye

ments of angular dependences for several crystal planes at each value of T. Since we do not have the capacities to accomplish this, we restricted ourselves to the most important parameters b_{20} and b_{22} and recorded spectra for only one orientation. Figure 3 shows the T-dependence of some EPR transitions in a typical sample at X-band frequencies for **B** || [001]. While the lines resulting from the axial species Fe4/2 and Fe6/2, and from some unidentified centers show constant resonance fields, the resonances on branches 1 and 3 of rhFe shift *continuously* with temperature [32]. This reflects the T-dependence of the Spin-Hamiltonian parameters for this center. Branches 2 and 4 are are lost for T > 180 K. With the help of Fig. 4, this feature may be understood easily. In this level diagram, drawn with the parameters listed in Tab. 1 for 75 K, the transitions are marked according to the branches of Fig. 3. One sees that transitions 2 and 4 occur between the levels of the Kramers doublet in the middle. They first run apart as the magnetic field increases, but then come close again. At approximately 180 K the maximum distance between these two levels corresponds to the energy of the microwave quanta. Transitions 2 and 4 will become broad and very sensitive towards temperature fluctuations. They will coincide and finally disappear. As four transitions are recorded for the given orientation below 180 K, one may obtain estimated parameters b_{20} and b_{22} in the following way: We omit the fourth-order spin-Hamiltonian parameters b_{4i}, which are not significant within our experimental precision (in contrast with Refs. [21, 23]), and furthermore set $g_x = g_y = g_z = 2$ (observed deviations from these values being small, see Tab. 1). Above 180 K, only two resolved resonances of rhFe are found (Fig. 3) and stable fits with two free paramters are no longer possible. The T-dependence of b_{20} and b_{22} obtained in this way is shown in Fig. 5. The validity of the applied procedure is supported by the fact that also the data points gained from angular scans (see Tab. 1) are compatible with the found dependences.

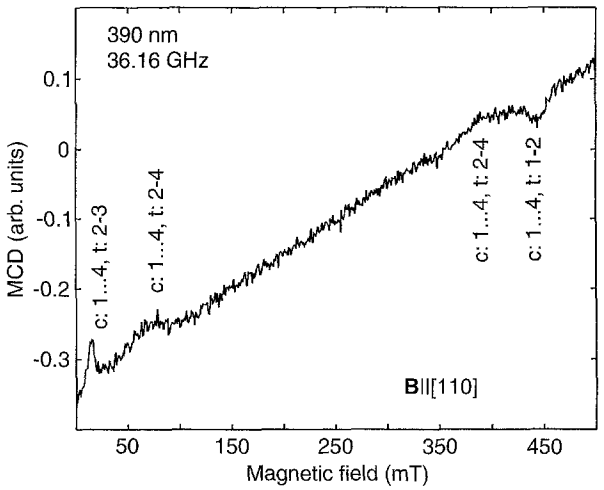

Fig. 6. MCD as a function of magnetic field B showing the ODMR lines of rhFe. The numbers of the center position 'c' refer to Fig. 4. By 't:2-3' a transition between levels 2 and 3 (numbered by increasing energy) is indicated. The approximately linear increase of the MCD with B reflects the growth of the spin polarization of the ground state. A negative zero field signal due to linear dichroism adds to the MCD. At resonance, both enhancement and decrease of |MCD| is observed (see text)

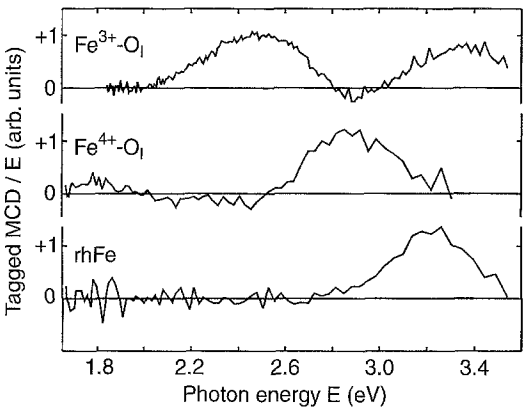

Fig. 7. Tagged-MCD spectra of rhFe, Fe_K^{3+}-O_I and axial Fe^{4+}. While the scales are indepedent and arbitrary, the signs of the signals correspond to those of normal MCD for each center

A rhFe center with temperature independent parameters $b_{20} = 0.44\,cm^{-1}$ and $b_{22} = 0.196\,cm^{-1}$ [23], which should be observable down to 4.2 K [21], can be ruled out in our samples. On the other hand these parameters, valid at 300 K, fit well to the T-dependence of the center observed at low temperatures. This makes it most plausible that only one rhFe center exists in $KTaO_3$. We will assume this for the rest of this paper.

2.2 MCD and ODMR

The MCD spectra of all our Fe-doped $KTaO_3$ crystals in the as-grown state were dominated by bands that we could relate earlier to Fe_K^{3+}-O_I centers using the tagged-MCD method [16]. The absorption related to this MCD leads at least partially to the brownish color of our Fe-doped samples. No MCD/ODMR signals from Fe4/2 could be found so far, although this center was easily visible by conventional EPR in all samples. We will comment on this finding in the last section. In thin samples ($\approx$ 1 mm) cut from lightly doped material (0.25 mol% Fe), where it is possible to measure down to 3.54 eV (350 nm), one finds in the near-UV spectral region ODMR lines at very low magnetic fields for 35 GHz, shown in Fig. 6. The resonances were observed for **B** || [110]. They can all be assigned to transitions in a level-diagram similar to that given in Fig. 4, when calculated with the parameters of rhFe that are valid at low temperatures. Also for 70 GHz the positions of the observed ODMR lines agree within a few mT with those of the calculated transitions. Finally, we could measure the angular dependence of some of these lines for the range $\varphi = 20°...70°(\vartheta = 90°)$ [33], the result being also fully compatible with calculations using the parameters valid at 4 K for rhFe (Tab. 1). Since we did not attempt to establish a model explaining the signs of the resonances, we must confine ourselves on stating that the only 'normal' ODMR-signal (decrease of |MCD|) corresponds to a transition beween the lowest Kramers-doublet. Such a transition *must* diminish the absolute value of the MCD, because oppositely signed MCD signals result from the two substates of a Kramers doublet. All the observed 'positive' or 'MCD- enhancing' ODMR signals are due to transitions between different Kramers doublets (split in zero field by b_{20} and b_{22}).

As indicated in the Figure, only resonances from one set of centers corresponding to the magnetically equivalent sites 1 to 4 (see Fig. 4, inset) are observable. Signals from a single site, 5 or 6, are expected at $\approx$30 mT and $\approx$50 mT according to the calculation, but are not resolved. Because the ODMR lines are this weak, it will be difficult to detect the optical orientation of rhFe in an analogous way as for Fe^{3+}-O_I [16]. There, the change of the relative intensity of the ODMR lines from magnetically inequivalent sites could be observed directly. Since in addition a substantial redistribution of the site occupancy by optical alignment is unlikely for rhFe [34], a considerable improvement of the experimental sensitivity would be needed to solve the question by ODMR, whether rhFe centers may be oriented optically as well.

The main result from the above is that all ODMR lines shown in Fig. 6 stem from transitions of rhFe. Having established this, one will obtain the MCD from rhFe, contributing additively to the total MCD, if one measures the height of a suitable resonance as a function of the wavelength, i.e., a tagged-MCD spectrum. The result is shown in Fig. 7. For comparison we also reproduced the tagged-MCD spectra of Fe_K^{3+}-O_I-ions [16] and axial Fe^{4+}-centers, presumably Fe_K^{4+}-O_I [35]. The sign of the MCD has been checked by proceeding as decribed elsewhere [36], since it may become important when a theoretical interpretation is attempted. However, the units are arbitrary and have been adjusted for each spectrum individually to normalize the height of the largest band.

The axial Fe^{4+}-centers can be generated metastably at low temperatures by an illumination-heating treatment as described in a recent publication [35]. By improving this treatment and thus increasing the number of Fe^{4+}-centers, we now could also measure the tagged-MCD of this defect. In a single scan, being displayed in the figure, the weak bands of the axial Fe^{4+}-centers are still barely larger than noise. Their existence and their shape has therefore been confirmed by repeated measurements and by direct observation of the cor-

responding ODMR signals at various wavelengths. The band at 1.8 eV, which was the only band that could be separated from the Fe_K^{3+}-O_I related features by simple MCD measurements [35], turns out to be rather small compared to a band at 2.9 eV. Being aware of the relation between MCD- and absorption bands [37], one may sketch qualitatively how the absorption spectrum of the Fe^{4+} centers may look like simply by giving the negative band (or bands) a positive sign: There will be a maximum at 2.9 eV, followed by one or two humps between 2.4 and 2.2 eV, and finally a weak band at 1.8 eV. This structure agrees surprisingly well with the spectra attributed to the oxygen-iron charge-transfer transition of Fe^{4+}-V_O and cubic Fe^{4+} in $SrTiO_3$ [38]. Also in $BaTiO_3$, the main absorption band of cubic Fe^{4+} was also found at 2.9 eV recently [39]. It remains to be clarified, why all these Fe^{4+} centers should exhibit rather similar spectra, although they possess partially very different local surroundings.

In contrast with this, we observe a strong influence of the local structure on the electronic properties in the MCD-spectra from the two observed Fe^{3+}-centers, Fe^{3+}-O_I and rhFe. Rhombic iron shows MCD- and, hence, absorption-bands only above 2.8 eV. This feature may be expected for the d^5- configuration of Fe^{3+}, where the low energy crystal field transitions are usually all spin-forbidden and extremly weak. Strong UV absorption bands of this ion result from ligand-to-metal charge transfer (LMCT) transitions. In MgO, perhaps the best known example from the class of oxides, an LMCT-band of Fe^{3+} peaks at 4.35 eV and shows a wing down to 3.7 eV [40]. A corresponding band in Al_2O_3 starts at 4 eV and peaks at 4.8 eV [41]. We therefore tentatively attribute the MCD-band of rhFe to the low-energy wing of an LMCT absorption band. Since the observed MCD band may be followed by a negative overlapping band at higher energies, the maximum at 3.25 eV does not necessarily indicate the peak of the corresponding absorption band, which may be located farther away in the UV region. In fact, a similar structure of the MCD, that is, a weak negative band followed by a strong positive one, was found for the just mentioned case of MgO [40]. The situation is completely different for Fe^{3+}-O_I, where MCD bands are observed down to the red spectral region. As mentioned, this is an unusual optical property of Fe^{3+} in a cubic host. It indicates that the electronic properties of the complex Fe^{3+}-O_I are strongly modified by the interstitial oxygen ion in comparison with Fe^{3+} centers possessing ligands from the host lattice only. Embedded cluster calculations are in progress, which should best be suited to test this assumption [42].

3 Summary and conclusions

In our experiments, the rhombic Fe^{3+}-center, rhFe, turned out to be one of the predominant iron centers in $KTaO_3$:Fe grown in oxidizing atmosphere. By estimating the dependence on temperature of the main parameters of the Spin-Hamiltonian of this defect, we showed that the low- and high-temperature EPR spectra, though looking rather different, belong to the same rhombic iron center. On this basis, the optical absorption in the visible and near UV of rhFe could be studied observing the MCD tagged by ODMR. Absorption has been found only in a narrow region below the band edge, in contrast with the tagged-MCD spectra of both Fe^{3+}-O_I and axial Fe^{4+}, which exhibit bands across almost the entire range of the visible spectral region. In connection with theoretical calculations, this finding should yield valuable information on the structure of this interesting center. Experimentally, ENDOR investigations are necessary to elucidate the nature of accompanying defects or structural rearrangements responsible for the lowering of symmetry. Measurements of this type are very promising, since for certain orientations of the magnetic field a partially resolved super-hyperfine structure may be observed for some EPR-transitions of rhFe [43].

We mentioned above, that we could not detect MCD and consequently ODMR signals from Fe4/2, although this center exhibits strong EPR lines in all our as-grown samples studied to date. One has to assume therefore, that Fe4/2 does not show substantial absorption and MCD bands in the spectral range investigated. This fact is rather surprising, because both candidates for this center, Fe^+ and Fe^{5+}, are expected to absorb in the visible. An LMCT band at 2.5 eV has been identified for Fe^{5+} in $SrTiO_3$ [44], and later, a photochromic band at 2.4 eV in $KTaO_3$:Fe was attributed the same transition by analogy [45]. To our knowledge, nothing is known about the optical properties of Fe^+ centers in oxide host crystals, but isoelectronic ions, like e.g. Co^{2+}, exhibit both charge transfer and, if the symmetry is lower than cubic, d-d transitions in the investigated spectral range. This fact seems to complicate the development of a defect model for the Fe4/2 center at the present stage.

Further experimental information on the nature of iron centers in $KTaO_3$ may be gained by redox-treatments of the crystals. Especially the MCD/ODMR properties of cubic Fe^{3+}, known to be generated by reduction in wet atmosphere [11], will be very interesting. If at all, this defect should exhibit absorption only in the near-UV spectral region, similar to rhFe.

Acknowledgement. We thank Professor Schirmer for fruitful discussions and active help. The support of the Deutsche Forschungsgemeinschaft, SFB 225, is gratefully acknowledged.

References

1. F. Agulló-López. editor: *Insulating Materials for Optoelectronics* (World Scientific, Singapore, 1995)
2. O.F. Schirmer, H.-J. Reyher, M. Wöhlecke: In *Insulating Materials for Optoelectronics*, ed. by F. Agulló-López (World Scientific, Singapore 1995), p. 93
3. D. Rytz, A. Châtelain, and U.T. Höchli: Phys. Rev. B **27**, 6830 (1983)
4. U.T. Höchli, K. Knorr, and A. Loidl: Adv. Phys. **39**, 405 (1990)
5. B.E. Vugmeister and M.D. Glinchuk: Rev. Mod. Phys. **62**, 993 (1990)
6. J.-M. Spaeth and F. Lohse: J. Phys. Chem. Solids **51**, 861 (1990)
7. K.W. Blazey and H. Weibel: J. Phys. Chem. Solids **45**, 917 (1984)
8. D.M. Hannon: Phys. Rev. **164**, 366 (1967)
9. G. Wessel and H. Goldick: J. Appl. Phys. **39**, 4855 (1968)
10. D. Rytz, U.T. Höchli, K.A. Müller, W. Berlinger, and L.A. Boatner: J. Phys. C: Solid State Phys. **15**, 3371 (1982)
11. R. Gonzales, M.M. Abraham, L.A. Boatner, and Y. Chen: J. Chem. Phys. **78**, 660 (1983)
12. S.Q. Fu, W.-K. Lee, A.S. Nowick, L.A. Boatner, and M.M. Abraham: J. Solid State Chem. **83**, 221 (1989)
13. I.P. Bykov, M.D. Glinchuk, A.A. Karmazin, and V.V. Laguta: Sov. Phys. Solid State **25**, 2063 (1983)

14. V.V. Laguta, M.D. Glinchuk, A.A. Karmazin, I.P. Bykov, and P.P. Syrnikov: Sov. Phys. Solid State **27**, 1328 (1985)
15. H. Donnerberg, M. Exner, and C.R.A. Catlow: Phys. Rev. B **47**, 14 (1993)
16. H.-J. Reyher, B. Faust, M. Käding, H. Hesse, E. Ruža, and M. Wöhlecke: Phys. Rev. B **51**, 6707 (1995), Phys. Rev. B, Erratum, submitted
17. M.M. Abraham, L.A. Boatner, D.N. Olson, and U.T. Höchli: J. Chem. Phys. **81**, 2528 (1984)
18. M.D. Glinchuk, V.V. Laguta, I.P. Bykov, J. Rosa, and L. Jastrabík: J. Phys.: Condens. Matter **7**, 2605 (1995)
19. M.D. Glinchuk, V.V. Laguta, I.P. Bykov, J. Rosa, and L. Jastrabík: Chem. Phys. Lett. **232**, 232 (1995)
20. V.V. Laguta, M.D. Glinchuk, I.P. Bykov, J. Rosa, L. Jastrabík, R.S. Klein, and G.E. Kugel: Phys. Rev. B **52**, 7102 (1995)
21. A.P. Pechenyi, M.D. Glinchuk, T.V. Antimirova, and W. Kleemann: Phys. Status Solidi B **174**, 325 (1992)
22. B. Salce, J.L. Gravil, and L.A. Boatner: J. Phys.: Condens. Matter **6**, 4077 (1994)
23. A.P. Pechenyi, M.D. Glinchuk, C.B. Azzoni, F. Scardina, and A. Paleari: Phys. Rev. B **51**, 12165 (1995)
24. B. Henderson and G.F. Imbusch: *Optical Spectroscopy of Inorganic Solids* (Clarendon, Oxford 1989)
25. H. Unoki and T. Sakudo: J. Phys. Soc. Japan **21**, 1730 (1966)
26. V.G. Grachev: Institute of Materials Sciences, 252180 Kiev, Ukraine
27. A. Abragam and B. Bleaney: *Electron Paramagnetic Resonance of Transition Ions* (Oxford University Press, Oxford 1970)
28. One may see from Fig. 1 and from Fig. 1 in [20] that the resonance from Fe4/2 at $\approx 320\,\mathrm{mT}$ is *above* the corresponding line from Fe6/2.
29. A. Abragam and M.H.L. Pryce: Proc. Roy. Soc. London A **206**, 164 and 173 (1951)
30. R.L. Berney and D.L. Cowan: Phys. Rev. B **23**, 37 (1981)
31. Th.W. Kool and M. Glasbeek: Solid State Commun. **22**, 193 (1977)
32. Two weakly temperature-dependent transitions of rhFe at 150 mT are superimposed by a strong resonance of Fe4/2 for $\mathbf{B} \parallel [001]$. Therefore these transitions are not suited to monitor rhFe [22], if signals from Fe4/2 are present at the same time.
33. The reflection from the surface of the crystal plate becomes anisotropic upon rotation. This destroys the MCD-signal.
34. Because of symmetry the projection of the polarization of the light, intended to achieve alignment, onto the local center axes cannot be chosen very differently for the various sites (see Fig. 4). Filling up only one site, for example, while depleting the others will therefore not be feasible, if rhFe can be aligned at all.
35. H.-J. Reyher, B. Faust, and O.F. Schirmer: Solid State Commun. **98**, 445 (1996)
36. H.-J. Reyher, R. Schulz, and O. Thiemann: Phys. Rev. B **50**, 3609 (1994)
37. P.J. Stephens: Advances in Chemical Physics Vol. **35**, Wiley, New York (1976), p. 197
38. O.F. Schirmer, W. Berlinger, and K.A. Müller: Solid State Commun. **16**, 1289 (1975)
39. M. Mazur and O.F. Schirmer: University of Osnabrück, to be published
40. F.A. Modine, E. Sonder, and R.A. Weeks: J. Appl. Phys. **48**, 3514 (1977)
41. H.H. Tippins: Phys. Rev. B **1**, 126 (1970)
42. H. Donnerberg: University of Osnabrück, private communication.
43. Hannon [8] reports on a similar finding of Wemple.
44. K.W. Blazey, O.F. Schirmer, W. Berlinger, and K.A. Müller: Solid State Commun. **16**, 589 (1975)
45. Y. Akishige and K. Ohi: Jap. J. Appl. Phys. **19**, 1633 (1980)

This article was processed by the author using the LaTeX style file *pljour2* from Springer-Verlag.